applied sciences

MDPI

Article

Terahertz-Wave Absorption Gas Sensing for Dimethyl Sulfoxide

Alec Passarelli [1], Timothy E. Rice [1], M. Arshad Zahangir Chowdhury [1], Megan N. Powers [1], Muhammad Waleed Mansha [2], Ingrid Wilke [3], Mona M. Hella [2] and Matthew A. Oehlschlaeger [1,*]

[1] Department of Mechanical, Aerospace, and Nuclear Engineering, Rensselaer Polytechnic Institute, Troy, NY 12180, USA
[2] Department of Electrical, Computer, and Systems Engineering, Rensselaer Polytechnic Institute, Troy, NY 12180, USA
[3] Department of Physics, Applied Physics, and Astronomy, Rensselaer Polytechnic Institute, Troy, NY 12180, USA
* Correspondence: oehlsm@rpi.edu

Featured Application: Gas Sensing.

Abstract: Gas sensing for dimethyl sulfoxide (DMSO) based on rotational absorption spectroscopy is demonstrated in the 220–330 GHz frequency range using a robust electronic THz-wave spectrometer. DMSO is a flammable liquid commonly used as a solvent in the food and pharmaceutical industries, materials synthesis, and manufacturing. DMSO is a hazard to human health and the work environment; hence, remote gas sensing for DMSO environmental and process monitoring is desired. Absorption measurements were carried out for pure DMSO at 297 K and 0.4 Torr (53 Pa). DMSO was shown to have a unique rotational fingerprint with a series of repeating absorption bands. The frequencies of transitions observed in the present study were found to be in good agreement with spectral simulations carried out based on rotational parameters derived in prior work. Newly, intensities of the rotational absorption lines were experimentally observed and reported for DMSO in this study. Measured intensities for major absorption lines were found in very good agreement with relative line intensities estimated by quantum mechanical calculations. The sensor developed here exhibited a detection limit of 1.3 10^{15}–2.6 10^{15} DMSO molecules/cm^3 per meter of absorption path length, with the potential for greater sensitivity with signal-to-noise improvements. The study illustrates the potential of all electronic THz-wave systems for miniaturized remote gas sensors.

Keywords: gas sensing; terahertz (THz); dimethyl sulfoxide; absorption; spectroscopy

Citation: Passarelli, A.; Rice, T.E.; Chowdhury, M.A.Z.; Powers, M.N.; Mansha, M.W.; Wilke, I.; Hella, M.M.; Oehlschlaeger, M.A. Terahertz-Wave Absorption Gas Sensing for Dimethyl Sulfoxide. Appl. Sci. **2022**, 12, 5729. https://doi.org/10.3390/app12115729

Academic Editor: Vincenzo Luigi Spagnolo

Received: 20 May 2022
Accepted: 31 May 2022
Published: 4 June 2022

1. Introduction

Terahertz-wave absorption spectroscopy offers the potential for quantitative and selective gas sensing for polar molecules in practical and harsh environments. Commercial electronic terahertz (THz) wave gas sensors may be realizable in the near term due to the fundamental advantages offered by absorption spectroscopy in the THz-wave region (0.1–1.0 THz or 3.33–33.3 cm ^{1}). This includes sensitivity, molecular selectivity, and strongly limited insensitivity to interference from water vapor and particle scattering compared to the infrared band, as well as the significant progress made in the development of THz-wave electronic sources and detectors that are miniaturized, robust, energy efficient, and inexpensive, relative to photonics devices. Due to these advantages, THz-wave gas sensing has shown recent success in analytical chemistry and engineering [1–8].

In recent studies, THz-wave absorption spectroscopy based on microelectronic sources and detectors has been used to probe rotational transitions for the detection of gaseous volatile organic compounds (VOCs) [9], halogenated hydrocarbons [10], cyanides [11,12],

small sulfur-containing compounds [13,14], and other chemical classes. However, there is minimal prior development of gas sensing for larger volatile sulfur compounds (VSCs).

Both organic and inorganic sulfur-containing compounds are used across a plethora of chemical, pharmaceutical, metallurgic, textile, photographic, food, and cosmetic applications [15]. VSCs are used in polymer and other material manufacturing and processing [16]. They are often used to affect the aromas of food and beverages, such as vegetables, cheese, coffee, chocolate, UHT milk, wine, and beer [17]. VSCs are naturally produced in the ocean by marine biota, making up approximately 40% of the sulfur emissions to the atmo-sphere [18].

Common VSCs include dimethyl sulfide and dimethyl sulfoxide (DMSO) [17]. See Figure 1 for the organic structure of DSMO ($H_3CS(O)CH_3$). DMSO is used in medical, cleaning, and polymer and paper manufacturing applications. It is used as an anti-inflammatory drug [19], for pain reduction, in healing wounds or injuries, and other conditions. DMSO, as part of medical treatments or as a natural component of various foods, is known to penetrate tissues, allowing for greater efficacy of drug treatments. DMSO is also used as an industrial solvent in fungicides, herbicides, and antibiotics, due to its antimicrobial activity. DMSO is used in clearing solutions where it acts as a solvent for the removal of organic and polymer debris from manufacturing and other equipment. It is also used in paint stripping applications and in material processing as a reaction and processing solvent during polymer manufacturing and casting and synthetic fiber production.

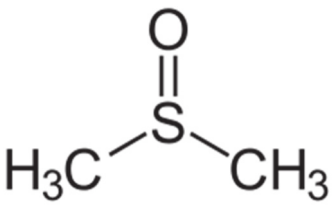

Figure 1. Molecular structure of DMSO.

A gas sensor for DMSO for process and environmental monitoring and control would be particularly valuable in industrial, manufacturing, materials, and medical settings, especially in situations where DMSO poses worker and environmental safety issues. For example, DMSO has been shown to lead to undesired exothermic reactions in medical settings, when exposed to sodium hydride [20]. In calorimetry experiments, DMSO/sodium hydride mixtures have been shown to lead to explosive conditions at very modest temperatures (40–60 C) [21]. Similarly, DMSO has been shown to decompose and act as an oxidizer or auto-catalyst while in contact with certain organic and inorganic acids and peroxides [22,23]. DMSO is a health hazard to humans causing skin/eye irritation and damage depending on exposure concentrations [24].

As a slightly asymmetric oblate top molecule with relatively strong dipole moment (3.94 Deybe [25]), DMSO proves to be a good candidate for gas-phase sensing using rotational absorption spectroscopy in the THz frequency band, where DMSO exhibits spectra rich in rotational structure from both the ground vibrational state and low-lying vibrationally-excited states [26,27]. Margules et al. [26] identified DMSO rotational transitions in the 150–660 GHz frequency range using high-resolution (10 kHz) methods carried out at very low pressures (0.2 Torr or 2.6 Pa) and presented a Watson Hamiltonian fit to describe the spectra. Cuisset et al. [27] extended the work of Margules et al. by adding transitions from low-lying vibrationally-excited states in the 70–700 GHz frequency band. Cuisset et al. also improved upon the Hamiltonian fit, providing updated rotational constants, including centrifugal distortion terms, for six vibrational ground states.

Several technologies have been used in the last several decades to investigate the rotational spectra of polar gas molecules in the THz-wave region. FAst Scan Submillimeter Spectroscopy Technique (FASSST) utilizes quasi-optical radiation sources and high-sensitivity and low time-response detectors, and it is most useful for highly resolved

spectral characterization (kHz resolution) at extremely low pressures where fast time response is not required [28–30]. While extremely resolved, FASSST systems are expensive, large, and slow, and, therefore, they are not suitable for remote gas sensing in industrial applications. THz time-domain spectroscopy (THz-TDS) provides greater time-resolution than FASSST and can scan large frequency ranges. However, typical THz-TDS systems do not have the spectral resolution of FASSST systems and may not provide a sufficient resolution for sensitive quantitative gas sensing under some conditions. THz-TDS systems are also generally too large, complex, and expensive to be implemented in remote gas sensing [1,2,31].

With advancements made to THz frequency microelectronic sources and detectors, miniature microelectronic THz-wave remote gas sensors are now possible that offer high time-resolution (seconds to milliseconds), offer reasonable spectral resolution (100 kHz to 1 MHz), are robust in industrial processes, and are inexpensive compared to other technologies. The present study presents the development of gas sensing for DMSO carried out using a THz-wave electronic spectrometer.

2. Experimental Methods

For the interrogation of rotational absorption spectra for the purposes of gas sensing, THz-wave radiation was generated with an electronic source, comprised of a radio frequency (RF) synthesizer (HP model 83,752, 10 MHz–20 GHz) coupled to a Virginia Diodes (VDi Model WR-3.4, power ~0.6 mW, resolution ~1 kHz, dimensions: 20 13 8 cm) signal generator extension (SGX) module that frequency multiplies the RF signal to generate THz-wave radiation. The output of the SGX module was coupled to a diagonal horn antenna to generate diverging free-space THz radiation. The diverging radiation was collimated using a plano-convex Teflon lens. The collimated radiation then passed through a high-density polyethylene (HDPE) gas cell assembled with two 45-degree HDPE windows. The absorption pathlength of the gas cell was 21.6 cm and was connected to a gas and vacuum management system. Downstream to the cell, a second plano-convex Teflon lens focused the radiation onto a Schottky diode detector (VDi Model QOD 3–15, sensitivity ~0.5 V/mW, NEP ~10 pW/rtHz, sub-ns time response, dimensions: 3.8 3.8 1.1 cm) for monitoring the transmitted radiation intensity. See Figure 2 for a schematic of the experimental hardware.

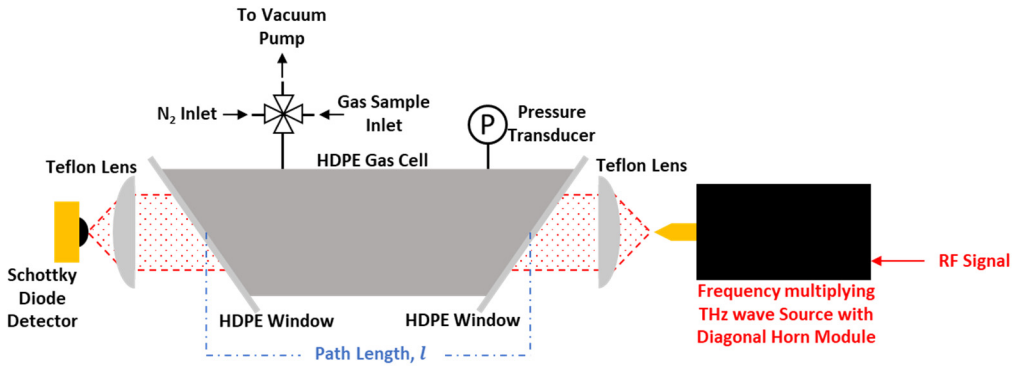

Figure 2. Schematic of the experimental setup.

The electronic source producing coherent radiation in a frequency range of 220–330 GHz was continuously scanned in frequency space at a fast rate (~100 GHz/s), providing rapid measurements that can also be averaged to increase the signal-to-noise ratio. The spectral absorbance, A, is described using the Beer-Lambert Law:

$$A = \#cl = \ln \frac{I}{I_0} \quad (1)$$

where # is the spectral absorption coefficient, c is the concentration of the absorbing gas (DMSO), and l is the absorption pathlength (21.6 cm). The reference and transmitted intensities are I_0 and I, respectively, where I_0 is measured while the cell is under vacuum and I is measured with the gas of interest in the cell. The absorption coefficient, #, is a function of the spectroscopic parameters for the probed absorption transitions (i.e., line position, strengths, and shapes), which are a function of frequency, temperature and pressure, and the gas mixture.

Spectral absorption for pure DMSO was measured at room temperature (297 K) and 0.4 Torr (53 Pa), using the methods described by Rice et al. [9]. First, a reference intensity was obtained by completing a frequency sweep of the radiation source while the gas cell was evacuated. To flush contaminants out of the gas cell, the cell was purged three times using pure N_2 and then evacuated with a turbomolecular pump prior to each experiment. Following the purge-vacuum process, the reference intensity was measured. Next, the cell was filled with DMSO, by vaporizing liquid DMSO (purity of 99.7+%) contained in attached glassware into the evacuated cell. DMSO has quite a low vapor pressure at room temperature (0.41 Torr (55 Pa) [32]); hence, measurements were carried out only at pressures of 0.4 Torr (53 Pa). Once the gas cell was filled, the radiation source was again swept in frequency, the transmitted intensity recorded, and the absorbance determined using the Beer-Lambert law. The signals for an example measurement are illustrated in Figure 3. The resulting absorbance measurements have a noise floor of approximately 10^{-3} in absorbance and have frequency resolution of 0.5 MHz.

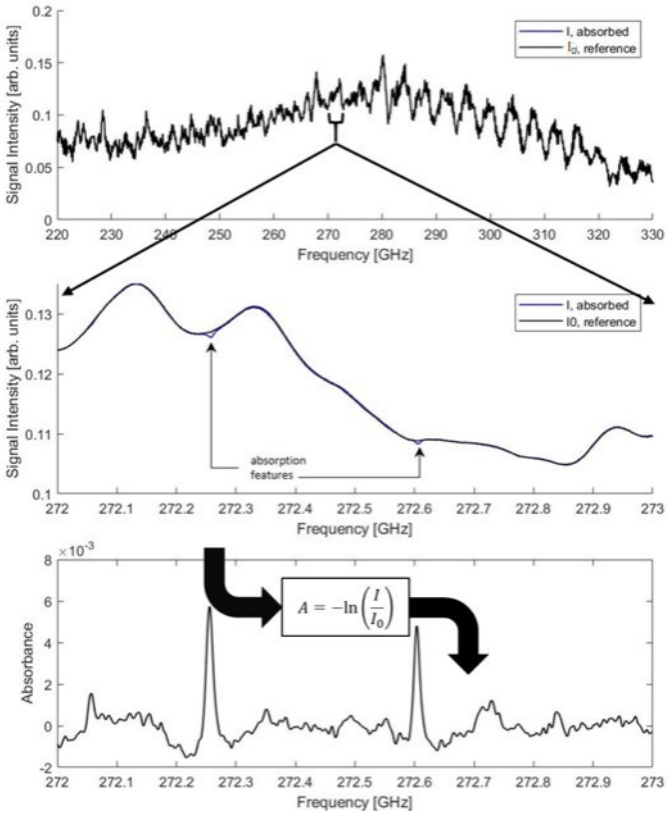

Figure 3. Example experiment: 0.4 Torr (53 Pa) pure DMSO at 297 K. Top panel: reference and absorbed intensity in total frequency range (220–330 GHz); middle panel: reference and absorbed intensity in subset of frequency range (272–273 GHz); bottom panel: absorbance in subset of frequency range.

3. Results and Discussion

Spectral absorbance measurements in the 220–330 GHz frequency range for pure DMSO at 297 K and 0.4 Torr (53 Pa) are illustrated in Figure 4. For the full frequency

range, repeating absorption bands (saw tooth structures) are observed with widths of ~2–3 GHz. The strength of the repeating bands increased from low to high frequency. At higher resolution, individual rotational lines were observed that make up the bands, and the strength of the lines generally increased within each repeating band from low to high frequency.

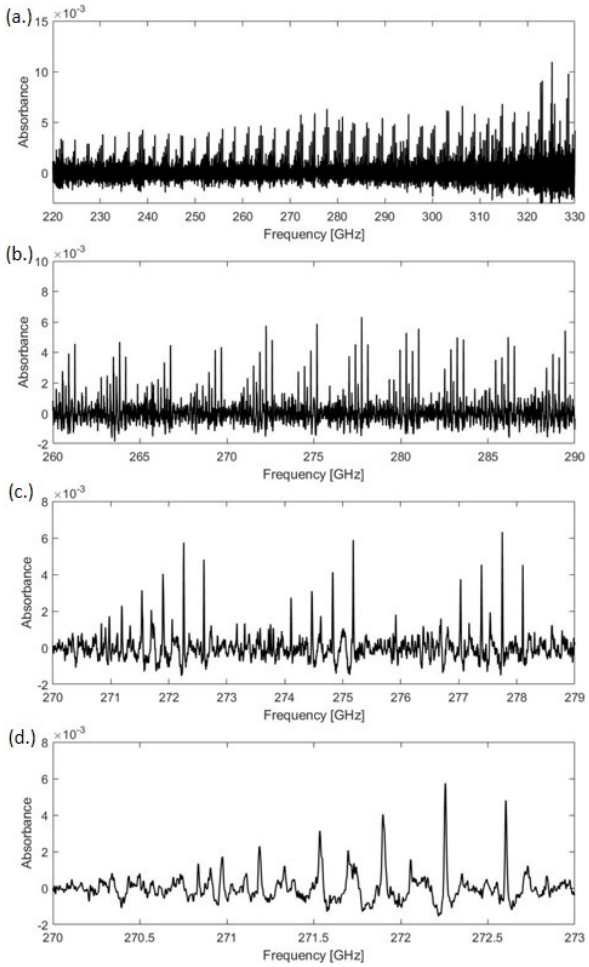

Figure 4. Measured absorbance for 0.4 Torr (53 Pa) pure DMSO at 297K in the frequency ranges of: (**a**) 220–330 GHz, (**b**) 260–290 GHz, (**c**) 270–279 GHz, and (**d**) 270–273 GHz.

Many distinct rotational lines were present within the repeating absorption bands, for both the ground vibrational state as well as for some low-lying vibrationally-excited states, as demonstrated by Margules et al. [26] and Cuisset et al. [27], who previously characterized the current frequency range in high-resolution low-pressure experiments (10 kHz, 0.2 Torr or 2.6 Pa). In the present experiments, carried out at higher pressures and for faster acquisition times necessary for remote gas sensing (1.1 s acquisition time in present study versus several hours in Cuisset et al.), 4–6 distinct transitions within each repeating feature were resolved against the noise floor. The noise floor (approximately 10^{-3} in absorbance space) contains broadband sensor noise, emanating from the THz source and detector, and weak unresolved rotational lines that provide structured features within the noise and are difficult to separate. Many of these weak unresolved lines are for five low-lying excited bending/vibrational states (200–400 cm^{-1}) [27] that contain fractions of DMSO molecules of order 10% at 297 K.

Margules et al. [26] and Cuisset et al. [27] carried out a fundamental characterization of DMSO rotational spectra in the 70–700 GHz range. In combination, those two studies identified and assigned approximately 7000 transitions but did not report intensities. Ad-

ditionally, Margules et al. and Cuisset et al. reported rotational constants and centrifugal distortion terms that allowed for prediction of the DMSO rotational spectrum. Here, calculations of the spectrum for DMSO in the ground-vibrational-state have been carried out using the PGOPHER code [33] with the rotational parameters reported by Cuisset et al. [27]. Comparisons of the predicted and measured spectrum are illustrated in Figures 5–7. As shown in Figures 6 and 7, the agreement is very good between the current measurements and the simulations for the strongest transitions observed here experimentally. Previous work [26,27] has reported precise measurement for the transition frequencies in the DMSO rotational spectra. Newly, intensities of the rotational absorption lines are experimentally observed and reported for DMSO in this study. Measured line intensities for major absorption lines are in very good agreement with relative line intensities predicted by the current quantum mechanical calculations.

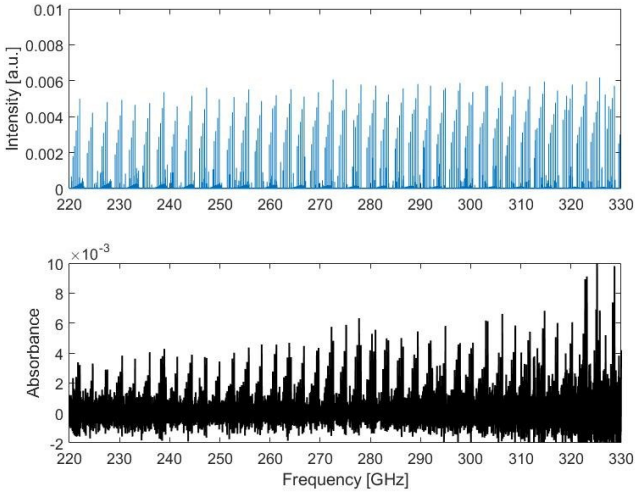

Figure 5. Comparison of measured absorbance (bottom) with line positions and intensities for the ground vibrational state simulated using PGOPHER [33] and the rotational constants of Cuisset et al. [27] in the total frequency range of current study (220–330 GHz).

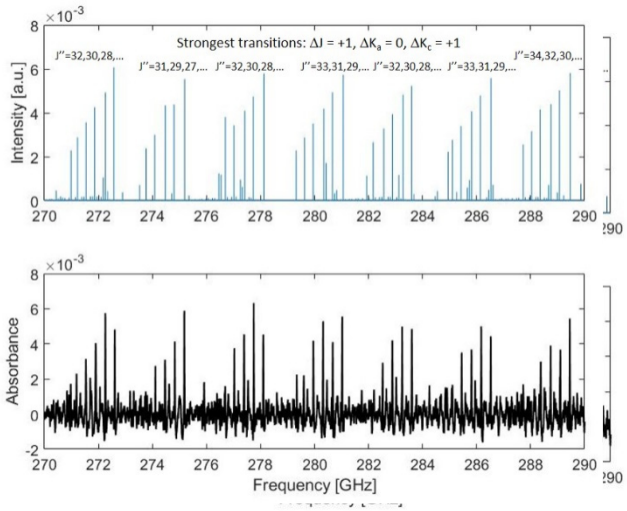

Figure 6. Comparison of measured absorbance (bottom) with line positions and intensities for the ground vibrational state simulated using PGOPHER [33] and the rotational constants of Cuisset et al. [27] in the 270–290 GHz frequency range.

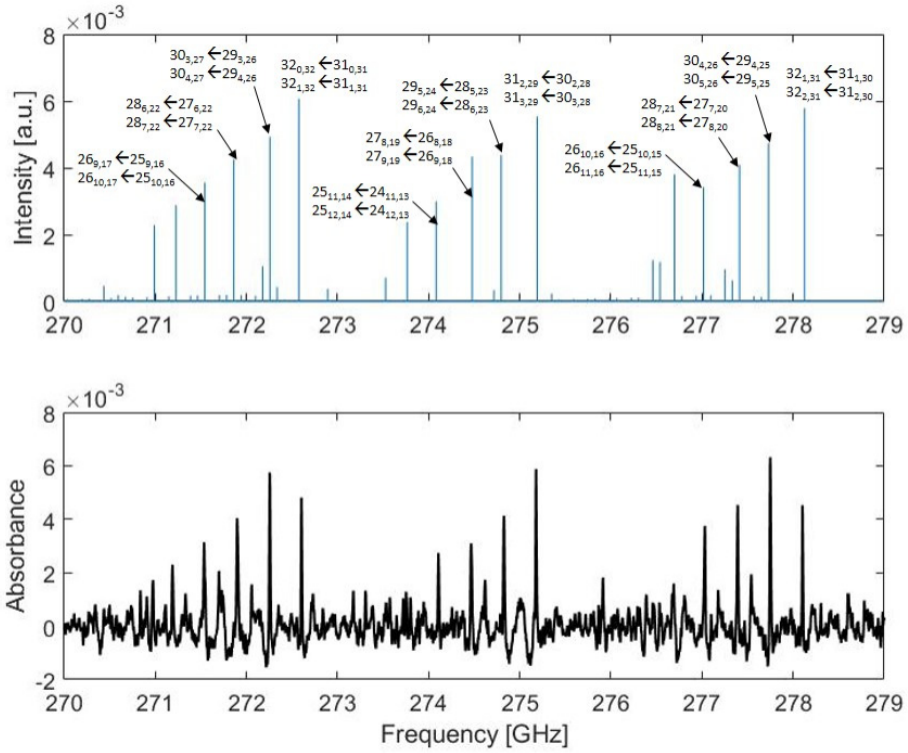

Figure 7. Comparison of measured absorbance (bottom) with line positions and intensities for the ground vibrational state simulated using PGOPHER [33] and the rotational constants of Cuisset et al. [27] in the 270–279 GHz frequency range.

DMSO is a slightly-asymmetric oblate top that has ground-vibrational-state rotational constants of A = 7036.58 MHz, B = 6910.83 MHz, and C = 4218.78 MHz [27]. As the PGOPHER simulations illustrate, the strongest transitions we observed in the present frequency range were a-type R-branch transitions, which obey the following selection rules: DJ = +1, DK_a = 0, and DK_c = +1, where J is the quantum number for overall angular momentum and K_a and K_c are the quantum numbers for the projection of angular momentum onto the a-axis and c-axis, respectively.

The repeating features observed in the rotational spectrum for DMSO exist because for each J" (lower state J), there is a series of K_c" (lower state K_c), described by K_c" = J", J" 1, J" 2, . . . 0, that are separated by approximately (A + B)/C = ~5.5 GHz, according to the energy level states participating in a-type R-branch transitions [34]. Each band is separated by approximately half of this separation value (~2.75 GHz) because each band begins with a different J". For example, as shown in Figure 7, the repeating bands between 270 and 279 GHz have the strongest features that alternate between J" = 31 and J" = 32. Within each repeating feature, the transitions are more tightly spaced, at around ~0.35 GHz, and the transitions exist in a sequence where the transitions are weaker at lower frequencies and weaker transitions are lower for J" and K_c". The spacing of transitions within a repeating band is a function of the rotational energy levels that results in neighboring transitions having J" that differ by two and K_c" that differ by five, i.e., these transitions exist for lower states that have quite different lower-state rotational energies, resulting in different transition intensities due to the differences in thermal populations.

The DMSO spectrum in the 220–330 GHz region exhibited spectral fingerprints, with the distinctive repeating patterns, that allow for the selective measurement of DMSO in the presence of other species, as there are many DMSO transitions to choose from. Most importantly, water vapor interference in the present frequency region is negligible and VOCs, that may be simultaneously present, have sparser spectra than DMSO [9], making it possible to find regions where DMSO is isolated. Given the proximity of DMSO lines to one another, low-pressure conditions are preferred for DMSO gas sensing, where line blending

due to pressure broadening is minimized. Here, we observed peak absorbance in each band that ranged from 0.005 to 0.01 for 0.4 Torr (53 Pa) of DMSO at 297 K and a 21.6 cm pathlength. Therefore, for a noise floor of 0.001 in absorbance, the DMSO detection limit is 1.3–2.6 10^{15} molecules/cm^3 per meter of absorption pathlength (50–100 ppm) for a 1.1 s acquisition time. It is possible, with slower frequency scan rates (~100 s acquisition time) and averaging/filtering techniques, to lower the noise floor by an order-of-magnitude or more, suggesting that detection limits of 10^{14} molecules/cm^3 per meter pathlength are possible for DMSO in the current frequency range.

4. Conclusions

THz-wave absorption spectroscopy for gas sensing of dimethyl sulfoxide (DMSO) was demonstrated using an electronic THz wave source and detector in a frequency range of 220–330 GHz at 297 K and 0.4 Torr (53 Pa). The measurements illustrate a distinctive DMSO absorption spectrum that exists as a series of repeating absorption bands. The current measurements agree with spectral simulations based on rotational constants derived in the prior work of Margules et al. [26] and Cuisset et al. [27]. The intensities of the rotational ab-sorption lines are experimentally observed and reported for DMSO between 220–330 GHz. Measured line intensities for major absorption lines are in very good agreement with relative line intensities estimated by quantum mechanical calculations. Detection limits for DMSO in the current frequency range are estimated to be in the range of 10^{14} to 10^{15} molecules/cm^3 per meter pathlength. Improvements to the sensor detection limits could be made through additional time averaging of signals, through either slower scan rates or multi-spectra averaging or frequency modulation methods. Remote gas sensing for DMSO has relevance to industrial, chemical, and medical applications where certain DMSO use conditions may lead to possible human health and environmental hazards. The present work shows the potential for remote gas sensing using THz-wave electronics for volatile sulfur compounds and other polar industrial chemicals.

Author Contributions: Conceptualization, A.P., T.E.R., M.M.H., I.W. and M.A.O.; methodology, A.P., T.E.R. and M.W.M.; investigation, A.P., T.E.R., M.A.Z.C. and M.N.P.; writing—original draft preparation, A.P.; writing—review and editing, I.W., M.M.H. and M.A.O.; supervision, I.W., M.M.H. and M.A.O. All authors have read and agreed to the published version of the manuscript.

Funding: This research was funded by the National Science Foundation, grant number CBET-185129.

Conflicts of Interest: The authors declare no conflict of interest.

References

1. Smith, R.M.; Arnold, M.A. Selectivity of Terahertz Gas-Phase Spectroscopy. Anal. Chem. **2015**, 87, 10679–10683. [CrossRef] [PubMed]
2. Hsieh, Y.-D.; Nakamura, S.; Abdelsalam, D.G.; Minamikawa, T.; Mizutani, Y.; Yamamoto, H.; Iwata, T.; Hindle, F.; Yasui, T. Dynamic Terahertz Spectroscopy of Gas Molecules Mixed with Unwanted Aerosol under Atmospheric Pressure Using Fibre-Based Asynchronous-Optical-Sampling Terahertz Time-Domain Spectroscopy. Sci. Rep. **2016**, 6, 28114. [CrossRef] [PubMed]
3. Yang, Y.; Shutler, A.; Grischkowsky, D. Measurement of the Transmission of the Atmosphere from 0.2 to 2 THz. Opt. Express **2011**, 19, 8830–8838. [CrossRef] [PubMed]
4. Dexheimer, S.L. Terahertz Spectroscopy: Principles and Applications; CRC Press: Boca Raton, FL, USA, 2017; ISBN 9781420007701.
5. Tekawade, A.; Rice, T.E.; Oehlschlaeger, M.A.; Mansha, M.W.; Wu, K.; Hella, M.M.; Wilke, I. Towards Realization of Quantitative Atmospheric and Industrial Gas Sensing Using THz Wave Electronics. Appl. Phys. B **2018**, 124, 105. [CrossRef]
6. Mansha, M.W.; Rice, T.E.; Oehlschlaeger, M.A.; Wilke, I.; Hella, M.M. A 220–300 GHz Twin-FET Detector for Rotational Spectroscopy of Gas Mixtures. IEEE Sens. J. **2021**, 21, 4553–4562. [CrossRef]
7. Mansha, M.W.; Wu, K.; Rice, T.E.; Oehlschlaeger, M.A.; Hella, M.M.; Wilke, I. Detection of Volatile Organic Compounds Using a Single Transistor Terahertz Detector Implemented in Standard BiCMOS Technology. In Proceedings of the 2019 IEEE SENSORS, Montreal, QB, Canada, 27–30 October 2019.
8. Neu, J.; Schmuttenmaer, C.A. Tutorial: An Introduction to Terahertz Time Domain Spectroscopy (THz-TDS). J. Appl. Phys. **2018**, 124, 231101. [CrossRef]
9. Rice, T.E.; Chowdhury, M.A.Z.; Mansha, M.W.; Hella, M.M.; Wilke, I.; Oehlschlaeger, M.A. VOC Gas Sensing Via Microelectronics-Based Absorption Spectroscopy at 220–330 GHz. Appl. Phys. B **2020**, 126, 152. [CrossRef]

10. Rice, T.E.; Chowdhury, M.A.Z.; Mansha, M.W.; Hella, M.M.; Wilke, I.; Oehlschlaeger, M.A. Halogenated Hydrocarbon Gas Sensing by Rotational Absorption Spectroscopy in the 220–330 GHz Frequency Range. Appl. Phys. B **2021**, 127, 123. [CrossRef]
11. Shimizu, N.; Ikari, T.; Kikuchi, K.; Matsuyama, K.; Wakatsuki, A.; Kohjiro, S.; Fukasawa, R. Remote Gas Sensing in Full-Scale Fire with Sub-Terahertz Waves. In Proceedings of the 2011 IEEE MTT-S International Microwave Symposium, Baltimore, MD, USA, 5–10 June 2011; pp. 1–4.
12. Rothbart, N.; Holz, O.; Koczulla, R.; Schmalz, K.; Hübers, H.-W. Analysis of Human Breath by Millimeter-Wave/Terahertz Spectroscopy. Sensors **2019**, 19, 2719. [CrossRef]
13. Hepp, C.; Luttjohann, S.; Roggenbuck, A.; Deninger, A.; Nellen, S.; Gobel, T.; Jorger, M.; Harig, R. A Cw-Terahertz Gas Analysis System with Ppm Detection Limits. In Proceedings of the 2016 41st International Conference on Infrared, Millimeter, and Terahertz waves (IRMMW-THz), Copenhagen, Denmark, 25–30 September 2016.
14. Khan, M.A.H.; Rao, M.V.; Li, Q. Recent Advances in Electrochemical Sensors for Detecting Toxic Gases: NO2, SO2 and H2S. Sensors **2019**, 19, 905. [CrossRef]
15. Shimada, T.; Takahashi, K.; Tominaga, M.; Ohta, T. Identification of Molecular Targets for Toxic Action by Persulfate, an Industrial Sulfur Compound. Neurotoxicology **2019**, 72, 29–37. [CrossRef] [PubMed]
16. Mutlu, H.; Ceper, E.B.; Li, X.; Yang, J.; Dong, W.; Ozmen, M.M.; Theato, P. Sulfur Chemistry in Polymer and Materials Science. Macromol. Rapid Commun. **2019**, 40, e1800650. [CrossRef] [PubMed]
17. Dziekońska-Kubczak, U.; Pielech-Przybylska, K.; Patelski, P.; Balcerek, M. Development of the Method for Determination of Volatile Sulfur Compounds (VSCs) in Fruit Brandy with the Use of HS–SPME/GC–MS. Molecules **2020**, 25, 1232. [CrossRef]
18. Yu, J.; Sun, M.-X.; Yang, G.-P. Occurrence and Emissions of Volatile Sulfur Compounds in the Changjiang Estuary and the Adjacent East China Sea. Mar. Chem. **2022**, 238, 104062. [CrossRef]
19. Talcott, P. Dcbt-Eim Equine Internal Medicine; Health Sciences: New York, NY, USA, 2018.
20. Olson, G.L. Lab Explosions. Chem. Eng. News **1966**, 44, 7.
21. Yang, Q.; Sheng, M.; Henkelis, J.J.; Tu, S.; Wiensch, E.; Zhang, H.; Zhang, Y.; Tucker, C.; Ejeh, D.E. Explosion Hazards of Sodium Hydride in Dimethyl Sulfoxide, N,N-Dimethylformamide, and N,N-Dimethylacetamide. Org. Process Res. Dev. **2019**, 23, 2210–2217. [CrossRef]
22. Deguchi, Y.; Kono, M.; Koizumi, Y.; Izato, Y.-I.; Miyake, A. Study on Autocatalytic Decomposition of Dimethyl Sulfoxide (DMSO). Org. Process Res. Dev. **2020**, 24, 1614–1620. [CrossRef]
23. Santosusso, T.M.; Swern, D. On the Mechanism of Oxidation of Epoxides by DMSO. Tetrahedron Lett. **1968**, 9, 4261–4264. [CrossRef]
24. Young, J.A. Dimethyl Sulfoxide. J. Chem. Ed. **2008**, 85, 629. [CrossRef]
25. Dreizler, H.; Dendl, G. Notizen: Rotationsspektrum, r0-Struktur Und Dipolmoment von Dimethylsulfoxyd. Z. Für Nat. A **1964**, 19, 512–514. [CrossRef]
26. Margulès, L.; Motiyenko, R.A.; Alekseev, E.A.; Demaison, J. Choice of the Reduction and of the Representation in Centrifugal Distortion Analysis: A Case Study of Dimethylsulfoxide. J. Mol. Spectrosc. **2010**, 260, 23–29. [CrossRef]
27. Cuisset, A.; Drumel, M.-A.M.; Hindle, F.; Mouret, G.; Sadovskií, D.A. Rotational Structure of the Five Lowest Frequency Fundamental Vibrational States of Dimethylsulfoxide. Chem. Phys. Lett. **2013**, 586, 10–15. [CrossRef]
28. Petkie, D.T.; Goyette, T.M.; Bettens, R.P.A.; Belov, S.P.; Albert, S.; Helminger, P.; De Lucia, F.C. A Fast Scan Submillimeter Spectroscopic Technique. Rev. Sci. Instrum. **1997**, 68, 1675–1683. [CrossRef]
29. Sieghard, A.; Petkie, D.T.; Bettens, R.P.A.; Belov, S.P.; De Lucia, F.C. FASSST: A New Gas-Phase Analytical Tool. Anal. Chem. **1998**, 70, 719A–727A.
30. De Lucia, F.C.; Petkie, D.T. THz Gas Sensing with Submillimeter Techniques. In Proceedings of the Terahertz for Military and Security Applications III, SPIE, Orlando, FL, USA, 18 May 2005; Volume 5790, pp. 44–53.
31. Kilcullen, P.; Hartley, I.D.; Jensen, E.T.; Reid, M. Terahertz Time Domain Gas-Phase Spectroscopy of Carbon Monoxide. J. Infrared Millim. Terahertz Waves **2015**, 36, 380–389. [CrossRef]
32. Fulem, M.; Růžička, K.; Růžička, M. Recommended Vapor Pressures for Thiophene, Sulfolane, and Dimethyl Sulfoxide. Fluid Phase Equilib. **2011**, 303, 205–216. [CrossRef]
33. Western, C.M.; Billinghurst, B.E. Automatic and Semi-Automatic Assignment and Fitting of Spectra with PGOPHER. Phys. Chem. Chem. Phys. **2019**, 21, 13986–13999. [CrossRef]
34. Cooke, S.A.; Ohring, P. Decoding Pure Rotational Molecular Spectra for Asymmetric Molecules. J. Spectrosc. **2012**, 2013, 698392. [CrossRef]